Published in final edited form as:
J Cell Physiol. 2007 January ; 210(1): 111–121. doi:10.1002/jcp.20828.

Distinctive Gene Expression of Prostatic Stromal Cells Cultured From Diseased Versus Normal Tissues

HONGJUAN ZHAO[1], **CRISTIANE F. RAMOS**[2], **JAMES D. BROOKS**[1], and **DONNA M. PEEHL**[1,*]

[1]Department of Urology, Stanford University, Stanford, California

[2]Urogenital Research Unit, State University of Rio de Janeiro, Brazil

Abstract

To obtain a comprehensive view of the transcriptional programs in prostatic stromal cells of different histological/pathological origin, we profiled 18 adult human stromal cell cultures from normal transition zone (TZ), normal peripheral zone (PZ), benign prostatic hyperplasia (BPH), and prostate cancer (CA) using cDNA microarrays. A hierarchical clustering analysis of 714 named unique genes whose expression varied at least threefold from the overall mean abundance in at least three samples in all 18 samples demonstrated that cells of different origin displayed distinct gene expression profiles. Many of the differentially expressed genes are involved in biological processes known to be important in the development of prostatic diseases including cell proliferation and apoptosis, cell adhesion, and immune response. Significance Analysis of Microarrays (SAM) analysis identified genes that showed differential expression with statistical significance including 24 genes between cells from TZ versus BPH, 34 between BPH versus CA, and 101 between PZ versus CA. S100A4 and SULF1, the most up- and downregulated genes in BPH versus TZ, respectively, showed expression at the protein level consistent with microarray analysis. In addition, sulfatase assay showed that BPH cells have lower SULF1 activity compared to TZ cells. Quantitative real-time polymerase chain reaction (qRT-PCR) analysis confirmed differential expression of ENPP2/autotoxin and six other genes between PZ versus CA, as well as differential expression of six genes between BPH versus CA. Our results support the hypothesis that prostatic stromal cells of different origin have unique transcriptional programs and point towards genes involved in actions of stromal cells in BPH and CA.

Stromal cells of the prostate are known to regulate epithelial growth as well as support and maintain epithelial function. Classic rodent studies have shown that stroma is a major inducer of epithelial cell growth and differentiation in prostate development by mediating androgen actions (Cunha, 1984; Cunha et al., 1987). These experiments demonstrated that prostatic development only occurs when embryonic stroma (Urogenital Sinus Mesenchyme (UGM), an androgen receptor-positive, mesodermally derived tissue) and epithelium (Urogenital Sinus Epithelium (UGE), an endodermally derived tissue) are recombined before implantation under the renal capsule of experimental animals, but not when implanted separately (Chung and Cunha, 1983; Cunha et al., 1983b). In addition, while wild-type UGM can induce urinary bladder epithelium to undergo a complete redifferentiation to a prostatic phenotype, androgen-insensitive UGM (which lacks the androgen receptor) fails to induce prostatic differentiation of UGE (Cunha et al., 1980; Cunha et al., 1983a).

*Correspondence to: Donna M. Peehl, Department of Urology, Stanford Medical Center, Stanford, CA 94305-5118. E-mail: dpeehl@stanford.edu

The stroma also plays an important role in the pathogenesis of prostate diseases (Cunha et al., 2002; Lee and Peehl, 2004; Chung et al., 2005). For instance, the earliest manifestation of benign prostatic hyperplasia (BPH) is the appearance of the mesenchyme in periurethral nodules, which has similar morphology to the prostatic mesenchyme during embryogenesis (McNeal, 1978). In later stages of BPH development, glandular budding and branching toward a central focus leads to further nodule growth (McNeal, 1978). Such morphological evidence suggests that BPH is intrinsically a mesenchymal disease that results from a reawakening of embryonic inductive interactions between the prostatic stroma and epithelium. In prostate cancer, the stroma generated by the recruiting signals released from adenocarcinoma cells, called "reactive stroma," is similar to the stroma at the sites of wound repair both histologically and molecularly (Tuxhorn et al., 2001; Chang et al., 2004; Condon, 2005). Reactive stroma from prostate cancer has been shown to stimulate cancer cell growth and migration and to promote angiogenesis by altering the balance of angiogenesis activators and inhibitors (Tuxhorn et al., 2002a,b). In addition, reactive stroma has been associated with the clinical course of prostate cancer, with increased reactive stroma predicting progression and worse outcome (Ayala et al., 2003). Finally, reactive stroma is capable of transforming a non-tumorigenic prostatic epithelial cell line (BPH-1) to a malignant one (Hayward et al., 2001). It becomes clear that the stroma in prostate cancer not only provides a supportive microenvironment that promotes tumor progression, but also is a critical determinant of benign versus malignant growth.

Despite the importance of stromal cells in prostate development, function and disease, a comprehensive view of the transcriptional programs in stromal cells of different histological and pathological origin is currently lacking. Such information may provide not only new insights into the biology of prostate pathogenesis, but also novel therapeutic strategies aimed at preventing the generation of stroma important for disease development and progression. For instance, genes comprising a stereotypical gene expression program in response to serum exposure by fibroblasts from 10 different anatomic sites have been shown to be coordinately regulated in many human tumors including prostate cancer (Chang et al., 2004). This transcriptional signature of the response of fibroblasts to serum has also been shown to be a powerful predictor of the clinical course in several common carcinomas.

Although prostatic stromal cells cultured from different histological and pathological origins are similar in certain phenotypic features including their morphology, population doubling time, cell cycle distribution, and response to genotoxic and chemotoxic agents, they differ in a number of aspects (San Francisco et al., 2004). First, carcinoma-associated fibroblasts (CAF) exhibit an increased potential to undergo anchorage-independent growth in soft agar compared to fibroblasts cultured from normal human prostate (NHPF) (San Francisco et al., 2004). Second, stromal cells from BPH (BPHF) and cancer tissues show different capability in inducing the growth of BPH-1 epithelial cells in tissue recombinant experiments (Barclay et al., 2005). BPH-1 recombinants with BPHF produced small grafts with similar histology to BPH. In contrast, CAF produced aggressive prostatic tumors when recombined with BPH-1 cells (Barclay et al., 2005). Finally, a number of molecules have been shown to be differentially expressed by stromal cells of different histology or pathology. For example, transforming growth factor (TGF)-β1 is expressed in higher concentrations in CAF than NHPF, which may contribute to the higher capability of CAF to form colonies in soft agar and the ability of CAF to promote malignant progression of prostate epithelial cells (San Francisco et al., 2004). In addition, a number of growth factors and cytokines are reportedly overexpressed in BPH stroma including fibroblast growth factor (FGF)-2, FGF-7, insulin-like growth factor (IGF)-1, IGF-2, and interleukin (IL)-1α (Lee and Peehl, 2004). Based on these observations, we hypothesize that prostatic stromal cells of different histological and pathological origins have distinct transcriptional programs. To test this hypothesis, we profiled 18 human stromal cell cultures from normal transition zone (TZ), normal peripheral zone (PZ), BPH, and cancer (CA) tissues

using cDNA microarrays containing 24,473 unique genes. We compared gene expression profiles of BPH cells to normal TZ cells because the TZ is the main site of origin of BPH. Similarly, we compared gene expression profiles of CA cells to normal PZ cells because the majority of prostate cancer arises in the PZ.

MATERIALS AND METHODS

Cell culture

Primary cultures of human prostatic stromal cells were established from histologically confirmed normal, BPH, or CA tissues according to previously described methods (Peehl and Sellers, 2000). The primary cell cultures used in this study are listed in Table 1. The presence of contaminating epithelial cells was ruled out by the absence of staining with antibodies against epithelial keratins 5 and 18 (Enzo Life Sciences, Inc., Farmingdale, NY). The stromal cell cultures were 100% pure by passage 2 under our culture conditions. These cultures were serially passaged in SCGM™ (Cambrex, East Rutherford, NJ) supplemented with 5 μg/ml insulin, 1 ng/ml FGF-2, 5% fetal bovine serum (FBS), and 100 μg/ml of gentamycin. At passages 4-17, cells were seeded on 100-mm cell culture dishes with 1 million cells/dish. Twenty-four hours later, cells were switched to MCDB 105 (Sigma-Aldrich, St. Louis, MO) with 100 μg/ml of gentamycin. Total RNA was isolated another 24 h later. MCF-7 cells were cultured in DMEM (Invitrogen™, Carlsbad, CA) supplemented with 10% FBS and MCF-10A cells were cultured in DMEM/F12 (Invitrogen™) supplemented with 15 mM HEPES buffer, 5% horse serum, 10 μg/ml insulin, 20 ng/ml epidermal growth factor (EGF), 100 ng/ml cholera toxin, and 0.5 μg/ml hydrocortisone.

RNA isolation and microarray hybridization

Total RNA was isolated using TRIzol solution (Invitrogen™) according to manufacturer's instructions. Fluorescently labeled DNA probes were prepared from 50 to 70 μg total RNA isolated from prostatic stromal cells (Cy5-labeled) and Universal Human Reference RNA (Stratagene, La Jolla, CA) (Cy3-labeled) by reverse transcription using an Oligo dT primer 50-TTTTTTTTTTTTTTT-30 (Qiagen, Valencia, CA) as described previously (Zhao et al., 2005). Labeled probes from each stromal cell RNA and reference RNA were mixed and hybridized overnight at 65°C to spotted cDNA microarrays with 41,126 elements (Stanford Functional Genomics Facility, Stanford, CA). Microarray slides were then washed to remove unbound probe and scanned with a GenePix 4000B scanner (Axon Instruments, Inc., Union City, CA).

Data processing and analysis

The acquired fluorescence intensities for each fluoroprobe were analyzed with GenePix Pro 5.0 software (Axon Instruments, Inc.). Spots of poor quality were removed from further analysis by visual inspection. Data files containing fluorescence ratios were entered into the Stanford Microarray Database (SMD) where biological data were associated with fluorescence ratios and genes were selected for further analysis (Sherlock et al., 2001). Hierarchical clustering was performed by first retrieving only spots with a signal intensity >150% above background in either Cy5- or Cy3 channels in at least 70% of the microarray experiments from SMD. We selected clones whose expression levels varied at least threefold in at least three of the samples from the mean abundance across all samples. The genes and arrays in the resulting data tables were ordered by their patterns of gene expression using hierarchical clustering analysis, and visualized using Tree-view software (http://rana.lbl.gov/EisenSoftware.htm). Genes with potentially significant differential expression in stromal cells from different histological/pathological origins were identified using the Significance Analysis of Microarrays (SAM) procedure, which computes a two-sample T-statistic (e.g., for BPH vs. TZ cells) for the normalized log ratios of gene expression levels for each gene (Tusher et al.,

2001). The procedure thresholds the T-statistics to provide a "significant" gene list and provides an estimate of the false discovery rate (the percentage of genes identified by chance alone). We used a selection threshold that gives a relatively low false discovery rate and identifies a relatively high number of significant genes.

Quantitative real-time PCR (qRT-PCR)

Total RNA from stromal cells was reverse transcribed as described above. cDNA product was then mixed with DyNAmo SYBR® Green master mix (Biolabs, Ipswich, MA) and primers of choice in the subsequent polymerase chain reaction (PCR) using a DNA Engine Opticon® 2 Continuous Fluorescence Detection System (MJ Research, Hercules, CA) according to manufacturer's instructions. Each reaction was done in triplicate to minimize the experimental variations (standard deviation was calculated for each reaction). Transcript levels of TATA box binding protein (TBP) were assayed simultaneously with each of the 35 genes selected for validation as an internal control to normalize their transcript levels. A list of the primer sequences used is available at http://genome-www5.stanford.edu/cgi-bin/tools/display/listMicroArrayData.pl?tableName=publication.

Immunochemistry

F-TZ-1 and F-BPH-4 cells cultured on 8-well chamber slides were fixed in 2% paraformaldehyde and permeabilized in 95% ice-cold ethanol. Horse serum (10% in phosphate-buffered saline (PBS)) was used to block non-specific binding of antibodies. The slide was then incubated at room temperature (RT) for 30 min in the primary antibody. A mouse monoclonal antibody against human SULF1 (CBI PGA antibody core, Tempe, Arizona) and a rabbit polyclonal antibody against S100A4 (Santa Cruz Biotechnology, Inc., Santa Cruz, CA) were used at a 1:50 dilution. The slides were then washed and incubated in a biotinylated secondary antibody at RT for 30 min, washed and incubated again at RT for another 30 min in peroxidase-conjugated streptavidin. Color was developed with 3′,3′ diaminobenzidine (DAB) (DakoCytomation California, Inc., Carpinteria, CA). Counter staining was performed with hematoxylin. A similar procedure was used for tissue sections, except that tissues were first deparaffinized in xylene, and hydrated in a graded series of alcohol. Slides were then incubated in 0.3% hydrogen peroxide in methanol for 15 min and 10% horse serum for 20 min at RT before incubation in the primary antibody at 4°C overnight.

Western blotting

Cells were lysed with lysis buffer (pH 7.5, 50 mM HEPES, 0.5% NP-40, 0.25% Na-deoxycholate, 0.1 mM sodium vanadate, 50 mM NaCl, 1 mM EDTA, 1 mM phenylmethylsulfonyl fluoride (PMSF)). Protein concentration was determined using the Bradford assay (Bio-Rad, Hercules, CA). Twenty micrograms of protein were separated using a 10% NuPAGE® 10% Bis-Tris Gel (Invitrogen) and transferred to a Hybond-P membrane (Amersham Life Sciences, Arlington Heights, IL). S100A4 was detected with a rabbit polyclonal anti-human antibody A5114 (DakoCytomation) and visualized with an ECL Plus kit (Amersham Biosciences, Piscataway, NJ). Glyceraldehyde-3-phosphate dehydrogenase (GAPDH) was detected with a monoclonal mouse anti-rabbit antibody, MoAb 6C5, which reacts with human GAPDH (Research Diagnostics, Flanders, NJ). S100A4 and GAPDH signal intensities were quantified with a Scion Image software (http://www.meyerinst.com/html/scion/scion_image_windows.htm).

In situ hybridization

In situ hybridization of tissue sections was performed based on a protocol published previously (West et al., 2004). Briefly, digoxigenin (DIG)-labeled sense and anti-sense RNA probes were

generated by in vitro transcription using templates produced by PCR amplification of a 498-bp product with the T7 promoter incorporated into the primers. In vitro transcription was performed with a DIG RNA-labeling kit and T7 polymerase according to the manufacturer's protocol (Roche Diagnostics, Indianapolis, IN). Tissue sections (5 μm) from paraffin blocks were digested in 10 μg/ml of proteinase K at 37°C for 30 min and hybridized overnight at 55° C with either sense or anti-sense riboprobes at 200 ng/ml dilution in mRNA hybridization buffer (DAKO). The following day, sections were incubated with a 1:35 dilution of RNase A cocktail (Ambion, Austin, TX) for 30 min at 37°C, followed by stringent washing. For signal amplification, a HRP-conjugated rabbit anti-DIG antibody (DAKO) was used to catalyze the deposition of biotinyl tyramide, followed by secondary streptavidin complex (GenPoint kit; DAKO). The final signal was developed with DAB (GenPoint kit; DAKO). For sense RNA probe, the primer sequences were 5′ CTAATACGACTCACTATAGGGATACTCGGCAGACACGTTCC3′ and 5′ CCTCCTTGAATGGGTGAAGA3′. For anti-sense RNA probe, the primer sequences were 5′ CTAATACGACTCACTATAGGGCCTCCTTGAATGGGTGAAGA3′ and 5′ ATACTCGGCAGACACG TTCC3′.

Sulfatase assay

F-TZ-1 or F-BPH-4 cells were cultured as described above and the assay was performed according to previously published protocols with modifications (Lai et al., 2004a). After 24 h in serum-free medium, cells were washed in ice-cold PBS and lysed in SIE buffer (250 mM sucrose, 3 mM imidazole, pH 7.4, 1% ethanol) containing 1% (w/v) Nonidet P-40 and 1 mM PMSF. Protein concentration was determined as described above. The total cellular protein (20 μg) was pre-incubated with 10 μM estrone-3-*O*-sulfamate (Sigma-Aldrich) at 37°C for 1 h to inhibit steroid sulfatases. 4-methylumbelliferyl sulfate was then added to a final concentration of 7.5 mM in a total volume of 200 μl. After incubation for 24 h at 37°C, the reaction was terminated by addition of 1 ml of 0.5 M Na_2CO_3/$NaHCO_3$, pH 10.7. The fluorescence of the liberated 4-methylumbelliferone was measured using excitation and emission wavelengths of 355 and 460 nm, respectively. MCF-7 and MCF-10A cells were used as positive and negative controls, respectively. Each reaction was performed in triplicate and standard deviation was calculated. The enzymatic activities of SULF1 in MCF-7, F-TZ-1, and F-BPH-4 cells were normalized against that in MCF-10A.

RESULTS

Gene expression profiles in prostatic stromal cells

We profiled gene expression of 18 stromal cell cultures including 4 from BPH, 2 from normal TZ, 5 from CA, and 7 from normal PZ (Table 1). In order to standardize culture conditions at the time of analysis, 1 million cells were inoculated into each of seven 100-mm dishes containing SCGM™. Twenty-four hours later, cells were changed to serum-free medium, then RNA was isolated 24 h later. This would allow the cells to enter a stationary, noncycling, or resting state, and minimize the differential gene expression due to different distributions of cells at each cell cycle phase. A hierarchical clustering analysis of 714 named unique genes represented by 1,032 clones whose expression varied at least threefold from the overall mean abundance in at least three samples in all 18 samples tested is shown in Figure 1A. In the dendrogram (Fig. 1B), BPH stromal cells were separated from normal TZ stromal cells, demonstrating that prostate stromal cells from normal TZ and BPH tissues have distinct gene expression patterns. CA stromal cells were grouped in a tight cluster away from cells from other histological/pathological origins except for one PZ stromal cell culture, indicating a unique transcriptional program associated with cancer-derived stromal cells. Note that two duplicate hybridizations of F-CA-1 clustered next to each other, showing a high reproducibility of the method. Interestingly, the PZ cultures showed heterogeneity in their gene expression

profiles, as they were broken into three groups by the clustering algorithm. F-PZ-1, -5, and -7 were similar to each other in their expression patterns, where as F-PZ-2, -3, and -4 were alike. F-PZ-6, on the other hand, showed a similar expression profile to CA cells for reasons other than misdiagnosis since the histology of the area of tissue where the cells came from was confirmed as normal. In addition, varying gene selection criteria did not change the association of samples significantly (Fig. 1C,D), suggesting a robust clustering. Of the named genes, more than 80% have some biological annotations associated according to Gene Ontology (GO). Many of them are involved in biological processes that are known to be important in the development of prostatic diseases including regulation of cell proliferation and apoptosis, cell adhesion, and immune response. See http://genome-www5.stanford.edu/cgi-bin/tools/display/listMicroArrayData.pl?tableName = publication for a complete list of genes.

Identification of genes differentially expressed using SAM analysis

The SAM procedure was used to identify genes with statistically significant differences in expression between groups of samples, because SAM accurately identifies transcripts with reproducible changes in gene expression and is more reliable than conventional means of analyzing microarrays (Tusher et al., 2001). Three comparisons were made between stromal cells of different histological/pathological origins. First, gene expression of BPH cells was compared to that of cells from TZ, the zone of origin of BPH. Thirty-four clones representing 24 unique named genes were selected by SAM as differentially expressed between TZ and BPH cells with a false positive rate of 24%. Of these, 21 were overexpressed in BPH compared to TZ cells, whereas 3 were underexpressed. Except for three of these genes, the others have been characterized to different extents according to GO annotations. The average-fold differences in expression of these genes between BPH versus TZ cells, ranks in SAM analysis, and GO annotations are listed in Table 2.

The next comparison was of genes expressed by stromal cells from the two different pathological diseases, BPH and cancer. Forty-eight clones representing 34 unique named genes were selected by SAM as differentially expressed between BPH and CA cells with a false positive rate of 13%. Of these, 28 were overexpressed in BPH cells compared to CA cells, whereas 6 were overexpressed in CA cells compared to BPH cells. Thirty of the 34 genes have biological annotations in GO. The average-fold differences in expression of these genes between BPH versus CA cells, ranks in SAM analysis, and GO annotations are listed in Table 3.

Finally, genes expressed by CA cells were compared to those expressed by normal cells from the PZ, the major zone of origin of adenocarcinomas in the prostate. One hundred seventeen clones representing 101 unique named genes were selected by SAM as differentially expressed between PZ and CA stromal cells with a false positive rate of 12%, all of which were overexpressed in CA compared to PZ cells. Sixty-eight genes that have biological annotations are listed in Table 4. The false positive rates of SAM analysis were relatively high, possibly due to the small sample sizes.

Validation of microarray data by qRT-PCR

To confirm the gene expression changes observed by microarray analysis, real-time RT-PCR was performed on selected genes identified by SAM analysis. We tested a total of 35 genes (14 for BPH vs. TZ, 7 for BPH vs. CA, and 14 for CA vs. PZ) using qRT-PCR, and determined the significance of differential expression by *t*-test (Table 5). We chose these genes because their known biological functions indicate that they may play a role in prostate pathogenesis. Nine of 14 genes (64%) were validated for the BPH versus TZ comparison, 6 of 7 genes (86%) for BPH versus CA, and 7 of 14 genes (50%) for CA versus PZ. As an example, relative

expression levels of SULF1 and S100A4, the most under- and overexpressed genes in BPH versus TZ cells, respectively, are shown in Figure 2. Expression of the top most differentially expressed genes in CA cells versus BPH cells, BST1 and OGN, were also confirmed (Fig. 2). These results demonstrated that the gene expression differences discovered by microarray analysis are reliable, especially for BPH versus TZ and BPH versus CA. The disagreement between qPCR and microarray data may be, in part, due to the differences in statistical methods (SAM vs. *t*-test).

SULF1 and S100A4 proteins are differentially expressed in BPH and TZ cells

SULF1 and S100A4 were the most under- or over-expressed genes in BPH compared to TZ cells, respectively, and have biological functions that indicate a possible role in disease development. To determine whether SULF1 and S100A4 were differentially expressed at the protein level, we performed immunochemistry on cultured BPH and TZ stromal cells. As shown in Figure 3, SULF1 expression was significantly less in F-BPH-4 compared to F-TZ-1 cells (Fig. 3E,F), whereas S100A4 expression was much higher in F-BPH-4 than in F-TZ-1 cells (Fig. 3G,H). Both cell cultures showed similar uniform expression of vimentin (Fig. 3A,B) and no staining when bovine serum albumin (BSA) was used as negative control (Fig. 3C,D). These results demonstrated that cultured BPH and TZ stromal cells differentially expressed these two genes not only at the transcript level, but also at the protein level.

Western blotting was performed to quantify the differences in S100A4 protein expression between cultured BPH and TZ stromal cells (Fig. 3I). A uniform upregulation of S100A4 protein expression in BPH cells was observed, ranging from 7.7- to 10.7-fold, compared to that in TZ cells. Moreover, protein expression of S100A4 was also increased in the stroma of BPH tissue (Fig. 4). Immunohistochemistry using paraffin-embedded tissue sections revealed intense staining of S100A4 throughout the stroma in the tissue of origin of F-BPH-4 cells (Fig. 4A,C), whereas only some stromal cells showed expression of S100A4 in tissue from which F-TZ-1 cells were cultured (Fig. 4B,D). These results showed that stromal cells cultured from BPH faithfully retained the high level of expression of S100A4 that was present in the tissue of origin.

Expression of SULF1 transcripts in tissue sections were examined by in situ hybridization since antibody against SULF1 protein did not work on paraffin-embedded tissues. TZ stroma displayed strong expression of SULF1 shown by anti-sense RNA probe staining (Fig. 4H), whereas little expression of SULF1 was detected in BPH stroma hybridized with the same probe (Fig. 4G). No staining was observed in the stroma of BPH (Fig. 4I) or TZ (Fig. 4J) tissue when sense RNA probe was used. These results confirmed our findings from microarray and real-time qPCR analyses and show that SULF1 is downregulated in BPH tissue as well as in stromal cells cultured from BPH.

SULF1 enzymatic activity is downregulated in BPH cells

To evaluate SULF1 protein activity in BPH and TZ stromal cells, we performed a functional assay to determine the enzymatic activity of SULF1 in whole cell lysates. The relative activity of SULF1 in TZ and BPH cells was calculated by normalization to the activity in the negative control, MCF-10A cells, in which no SULF1 transcript is detectable. MCF-7 cells, previously shown to possess SULF1 activity, were used as a positive control. A more than fourfold decrease in SULF1 activity was observed in F-BPH-4 cells compared to F-TZ-1 cells (Fig. 5), consistent with the decrease in SULF1 transcript in F-BPH-4 cells shown by microarray and qRT-PCR. These results demonstrate that SULF1 is downregulated in BPH cells at both transcript and protein function levels.

DISCUSSION

Prostatic stromal cells cultured from tissues of different histological and pathological origins displayed distinct gene expression profiles. Many of the differentially expressed genes are involved in biological processes known to be important in the development of prostatic diseases including regulation of cell proliferation and apoptosis, cell adhesion, and immune response. SAM analysis identified genes that showed differential expression with statistical significance between two classes of samples with relevant histopathology. Our results provide a comprehensive evaluation of the gene expression profiles of cultured prostatic stromal cells, and support the hypothesis that prostatic stromal cells of different histological/pathological origins are indeed different in their transcriptional programs. This dataset also serves as a valuable resource for researchers to explore the mechanisms of actions of stromal cells in the development of BPH and prostate cancer. It should be noted that although expression of certain genes such as FGFs and FGF receptor subtypes by cultured prostatic stromal cells seems to mimic the expression pattern in tissue quite faithfully, primary stromal cells growing on plastic do not represent conditions that mimic stromal-epithelial interactions. Therefore, caution needs to be taken when interpreting gene expression data generated using cultured cells, especially if cells are of relatively high passage and will have undergone significant change in their gene expression profiles.

Almost all prostate gene expression profiling studies have focused on molecular events associated with abnormalities in epithelial cells using either whole tissues or cultured cells (Luo et al., 2001; Brooks, 2002; Fromont et al., 2004; Nelson, 2004; Rose et al., 2005). We previously conducted one of the few gene expression profiling studies to date of prostatic stromal cells in which we investigated doxazosin-induced gene expression (Zhao et al., 2005). In that study, we only evaluated two cultures of each normal and pathological type (TZ and BPH), but nevertheless observed similar partitioning of normal TZ stromal cells from BPH stromal cells based on their gene expression patterns. In fact, when hierarchical clustering was performed using combined data for TZ and BPH cultures from our previous and current studies, a clear separation of TZ from BPH cells was observed (unpublished data), indicating a robust difference between transcription programs in BPH versus normal TZ stromal cells. Out of the 34 clones selected by SAM as differentially expressed between TZ and BPH cells in this study, 69% also showed differential expression in the same direction in our previous dataset. This finding also demonstrates the high reproducibility of our microarray experiments.

We compared our results with those in a recently published report by Joesting et al. (2005) of genes differentially expressed between cultures of prostate cancer-associated fibroblasts (CAFs) and normal-associated fibroblasts (NAFs) using Affymetrix microarrays. In that study, 119 genes were identified with a statistically significant difference in expression between CAFs and NAFs. We found no overlap of those 119 genes with the 101 genes that we identified as differentially expressed between CA stromal cells and normal PZ stromal cells. In addition, we examined the expression of SFRP1, identified in the study by Joesting et al. (2005) as overexpressed in CAF compared to NAF and suggested to be a candidate mediator of stromal-to-epithelial signaling in prostate cancer. Our microarray analysis showed no significant difference in the expression level of SFRP1 between CA and PZ stromal cells (P=0.06). We also measured SFRP1 mRNA in CA and PZ stromal cells by real-time qPCR and again found no significant difference in expression (P=0.28) (not shown).

There are several possible explanations for the differences in genes identified in these two studies. First, and may be the most important, is that the normal stromal cells used in these two studies were perhaps different. Ours come exclusively from histologically defined PZ of the prostate, whereas the study by Joesting et al. (2005) used NAFs from undefined zonal areas. When we compared gene expression between CA stromal cells and normal stromal cells from

TZ or central zone (CZ), the genes identified did not overlap with those found when normal PZ cells were used in the comparison (not shown). It appears that the anatomic origin of normal stromal cells is an important factor in such comparisons and caution needs to be taken when interpreting results from incompletely characterized cells or tissues. This is consistent with the finding of Stamey et al. (2003) who noted that different gene profiles were identified when cancer tissues were compared to normal tissues depending on which of the three zonal tissues (CZ, PZ, or TZ) were used as a control. Another explanation for the different results may be the phenotypic state of the cells at the time of RNA isolation. In order to eliminate complexities related to relative states of confluency, proliferation, and differentiation among the cell cultures, we followed a strict protocol of inoculating a given number of cells into non-proliferative (serum-free) medium 24 h prior to RNA extraction. Certainly different protocols may have a significant impact on gene expression profiles. Alternatively, differences in the array platforms and statistical methods used to derive the gene lists may also contribute to the differences observed.

Novel genes that showed differential expression between stromal cells of BPH and TZ in our study should shed light on the role of stromal cells in the pathogenesis of BPH. The current theory is that autocrine and paracine signaling from stromal cells creates a focal area of reawakening of epithelial budding and BPH nodule formation. Although a number of factors have been implicated as mediators of such autocrine and paracrine signaling including FGF, EGF, IGF, and TGF-β, the precise mechanisms that cause BPH are not clear (Lee and Peehl, 2004). Our results implicate the decreased expression of a factor, SULF1, as an important event leading to enhanced growth factor signaling in BPH. Several studies have shown that SULF1, a cell surface sulfatase, functions as a negative regulator of cell growth and that loss of SULF1 potentiates signaling of growth factors such as hepatocyte growth factor (HGF) and FGF (Lai et al., 2003, 2004a,b; Wang et al., 2004). We propose that loss of SULF1 in prostate stromal cells exerts a pro-proliferative effect in an autocrine and/or paracrine manner that leads to an overgrowth of epithelial and stromal cells. In addition, loss of SULF1 may also be related to the decreased apoptosis in BPH that has been reported (Lee and Peehl, 2004), since such an effect of decreased SULF1 expression has been reported in a number of tissues (Lai et al., 2004a,b; Sala-Newby et al., 2005).

The theory of embryonic “reawakening” in the pathogenesis of BPH states that BPH is a process of epithelial budding and branching similar to the glandular morphogenesis that occurs in embryonic tissue as a result of stimulation from the underlying mesenchymal tissue (Isaacs and Coffey, 1989). Consistent with this theory, we observed overexpression of genes that are known components of important signaling pathways in embryonic development of the prostate. It has been shown that during ductal bud formation in rat prostate, activities of Sonic hedgehog (Shh) pathway components including the Shh receptor, Ptc1, and the members of the Gli gene family of transcriptional regulators (Gli1, Gli2, and Gli3) play a role in prostatic epithelial growth through epithelial-stromal interactions (Lamm et al., 2002; Lipinski et al., 2005). For instance, expression of Gli1, Gli2, and Gli3 was detected in the UGM during this period (Lamm et al., 2002). We observed a strong upregulation of Gli3 at the transcript level in BPH compared to normal TZ stromal cells, suggesting a possible role of Shh signaling in promoting overgrowth of prostatic epithelium, stroma, or both in BPH nodule formation. Further investigation of the expression of target genes of the Shh pathway in BPH will help to determine the scope of involvement of Shh signaling in the pathogenesis of BPH.

Besides providing evidence to support existing theories of BPH formation, our study also provides new insights into the mechanisms that may underlie this pathological process. For instance, we observed an upregulation of S100A4, a member of the S100 calcium-binding protein family, at both transcript and protein level in BPH compared to normal TZ stromal cells. This protein, also known as FSP1 (fibroblast-specific protein 1), is expressed by

fibroblasts, possibly derived from epithelial cells through epithelial-mesenchymal transformation, during experimental tissue fibrosis (Strutz et al., 1995; Iwano et al., 2002). Its expression is also inducible by cytokines classically associated with fibrosis including EGF and TGF-β1 (Okada et al., 1997). In addition, experimental fibrogenesis can be attenuated by the selective elimination of tissue fibroblasts using a herpes virus thymidine kinase transgene under the control of the FSP1 promoter (Iwano et al., 2001). These findings provided direct evidence that FSP1-expressing fibroblasts play a crucial role in the progression of fibrosis. The upregulation of FSP1 in BPH stromal cells that we observed indicates that molecular mechanisms underlying fibrosis may be involved in the pathogenesis of BPH. There is a large body of evidence that in BPH, the stromal-to-epithelial ratio increases up to 5:1 compared to the normal ratio of 2:1, and early nodules in the periurethral area are mostly stromal (McNeal, 1990; Shapiro et al., 1992). It is possible that this increase in the stromal volume is a result of fibrogenesis similar to that in fibrosis, and that blocking fibrosis may be effective in BPH treatment.

It is becoming accepted that the stromal microenvironment contributes to tumorigenesis in cancers of epithelial origin, including prostate cancer (Cunha et al., 2002, 2003). There are a number of molecular mediators of stromal-epithelial interactions in tumorigenesis reported so far. Our study implicates ENPP2/autotaxin and lysophosphatidic acid (LPA) signaling in stromal-epithelial interaction in prostate cancer. Autotaxin has been shown to be a potent stimulator of cancer cell motility and angiogenesis, an anti-apoptotic factor in mouse fibroblasts, and a specific target of transformation by v-JUN in chicken fibroblasts (Nam et al., 2001; Umezu-Goto et al., 2002; Black et al., 2004; Hama et al., 2004; Song et al., 2005). Because autotaxin is a key enzyme responsible for LPA generation in vivo, the observed functions of autotaxin are likely to be mediated by LPA signaling, which has been implicated in such diverse processes as wound healing, vascular remodeling, and tumor progression (Brindley, 2004; Moolenaar et al., 2004). In our study, SAM analysis showed that autotaxin is the most differentially expressed gene between CA and normal PZ stromal cells, and qRT-PCR confirmed its overexpression in CA stromal cells. This overexpression may have two consequences in the development of prostate cancer. First, autotaxin may act as an autocrine signal to promote stromal proliferation, a key element in creation of a “reactive stroma.” In addition, since autotaxin is a secreted protein, it also may act as a paracrine factor in stimulating epithelial growth and angiogenesis in cancer tissues. Our findings suggest that autotaxin may be a valuable target in interventions to eliminate stromal contributions in tumor progression.

Taken together, our dataset may serve as a valuable resource for exploring molecular mechanisms underlying prostate pathogenesis. Such knowledge may also help the discovery of therapeutic targets for treatment of BPH and cancer.

ACKNOWLEDGMENTS

Hongjuan Zhao is supported by the David W. Packard gift fund for GU Oncology. Cristiane F. Ramos is a fellow of CNPq (National Council of Scientific and Technological Development).

Contract grant sponsor: Department of Defense; Contract grant number: W81XWH-04-1-0810.

LITERATURE CITED

Ayala G, Tuxhorn JA, Wheeler TM, Frolov A, Scardino PT, Ohori M, Wheeler M, Spitler J, Rowley DR. Reactive stroma as a predictor of biochemical-free recurrence in prostate cancer. Clin Cancer Res 2003;9(13):4792–4801. [PubMed: 14581350]

Barclay WW, Woodruff RD, Hall MC, Cramer SD. A system for studying epithelial-stromal interactions reveals distinct inductive abilities of stromal cells from benign prostatic hyperplasia and prostate cancer. Endocrinology 2005;146(1):13–18. [PubMed: 15471963]

Black EJ, Clair T, Delrow J, Neiman P, Gillespie DA. Microarray analysis identifies Autotaxin, a tumour cell motility and angiogenic factor with lysophospholipase D activity, as a specific target of cell transformation by v-Jun. Oncogene 2004;23(13):2357–2366. [PubMed: 14691447]

Brindley DN. Lipid phosphate phosphatases and related proteins: Signaling functions in development, cell division, and cancer. J Cell Biochem 2004;92(5):900–912. [PubMed: 15258914]

Brooks JD. Microarray analysis in prostate cancer research. Curr Opin Urol 2002;12(5):395–399. [PubMed: 12172426]

Chang HY, Sneddon JB, Alizadeh AA, Sood R, West RB, Montgomery K, Chi JT, van de Rijn M, Botstein D, Brown PO. Gene expression signature of fibroblast serum response predicts human cancer progression: Similarities between tumors and wounds. PLoS Biol 2004;2(2):E7. [PubMed: 14737219]

Chung LW, Cunha GR. Stromal-epithelial interactions: II. Regulation of prostatic growth by embryonic urogenital sinus mesenchyme. Prostate 1983;4(5):503–511. [PubMed: 6889194]

Chung LW, Baseman A, Assikis V, Zhau HE. Molecular insights into prostate cancer progression: The missing link of tumor microenvironment. J Urol 2005;173(1):10–20. [PubMed: 15592017]

Condon MS. The role of the stromal microenvironment in prostate cancer. Semin Cancer Biol 2005;15 (2):132–137. [PubMed: 15652458]

Cunha, GR. Androgenic effects upon prostatic epitheliium are mediated via trophic influences from stroma. In: Kimball, FA.; Stein, Gary; Car, DB., editors. New approaches to the study of benign prostatic hyperplasia. Liss; New York: 1984. p. 81-102.

Cunha GR, Reese BA, Sekkingstad M. Induction of nuclear androgen-binding sites in epithelium of the embryonic urinary bladder by mesenchyme of the urogenital sinus of embryonic mice. Endocrinology 1980;107(6):1767–1770. [PubMed: 7428691]

Cunha GR, Fujii H, Neubauer BL, Shannon JM, Sawyer L, Reese BA. Epithelial-mesenchymal interactions in prostatic development. I. morphological observations of prostatic induction by urogenital sinus mesenchyme in epithelium of the adult rodent urinary bladder. J Cell Biol 1983a;96 (6):1662–1670. [PubMed: 6853597]

Cunha GR, Sekkingstad M, Meloy BA. Heterospecific induction of prostatic development in tissue recombinants prepared with mouse, rat, rabbit and human tissues. Differentiation 1983b;24(2):174–180. [PubMed: 6884617]

Cunha GR, Donjacour AA, Cooke PS, Mee S, Bigsby RM, Higgins SJ, Sugimura Y. The endocrinology and developmental biology of the prostate. Endocr Rev 1987;8(3):338–362. [PubMed: 3308446]

Cunha GR, Hayward SW, Wang YZ. Role of stroma in carcinogenesis of the prostate. Differentiation 2002;70(910):473–485. [PubMed: 12492490]

Cunha GR, Hayward SW, Wang YZ, Ricke WA. Role of the stromal microenvironment in carcinogenesis of the prostate. Int J Cancer 2003;107(1):1–10. [PubMed: 12925950]

Fromont G, Chene L, Latil A, Bieche I, Vidaud M, Vallancien G, Mangin P, Fournier G, Validire P, Cussenot O. Molecular profiling of benign prostatic hyperplasia using a large scale real-time reverse transcriptase-polymerase chain reaction approach. J Urol 2004;172(4 Pt 1):1382–1385. [PubMed: 15371850]

Hama K, Aoki J, Fukaya M, Kishi Y, Sakai T, Suzuki R, Ohta H, Yamori T, Watanabe M, Chun J, Arai H. Lysophosphatidic acid and autotaxin stimulate cell motility of neoplastic and non-neoplastic cells through LPA1. J Biol Chem 2004;279(17):17634–17639. [PubMed: 14744855]

Hayward SW, Wang Y, Cao M, Hom YK, Zhang B, Grossfeld GD, Sudilovsky D, Cunha GR. Malignant transformation in a nontumorigenic human prostatic epithelial cell line. Cancer Res 2001;61(22): 8135–8142. [PubMed: 11719442]

Isaacs JT, Coffey DS. Etiology and disease process of benign prostatic hyperplasia. Prostate Suppl 1989;2:33–50. [PubMed: 2482772]

Iwano M, Fischer A, Okada H, Plieth D, Xue C, Danoff TM, Neilson EG. Conditional abatement of tissue fibrosis using nucleoside analogs to selectively corrupt DNA replication in transgenic fibroblasts. Mol Ther 2001;3(2):149–159. [PubMed: 11237671]

Iwano M, Plieth D, Danoff TM, Xue C, Okada H, Neilson EG. Evidence that fibroblasts derive from epithelium during tissue fibrosis. J Clin Invest 2002;110(3):341–350. [PubMed: 12163453]

Joesting MS, Perrin S, Elenbaas B, Fawell SE, Rubin JS, Franco OE, Hayward SW, Cunha GR, Marker PC. Identification of SFRP1 as a candidate mediator of stromal-to-epithelial signaling in prostate cancer. Cancer Res 2005;65(22):10423–10430. [PubMed: 16288033]

Lai J, Chien J, Staub J, Avula R, Greene EL, Matthews TA, Smith DI, Kaufmann SH, Roberts LR, Shridhar V. Loss of HSulf-1 up-regulates heparin-binding growth factor signaling in cancer. J Biol Chem 2003;278(25):23107–23117. [PubMed: 12686563]

Lai JP, Chien J, Strome SE, Staub J, Montoya DP, Greene EL, Smith DI, Roberts LR, Shridhar V. HSulf-1 modulates HGF-mediated tumor cell invasion and signaling in head and neck squamous carcinoma. Oncogene 2004a;23(7):1439–1447. [PubMed: 14973553]

Lai JP, Chien JR, Moser DR, Staub JK, Aderca I, Montoya DP, Matthews TA, Nagorney DM, Cunningham JM, Smith DI, Greene EL, Shridhar V, Roberts LR. hSulf1 sulfatase promotes apoptosis of hepatocellular cancer cells by decreasing heparin-binding growth factor signaling. Gastroenterology 2004b;126(1):231–248. [PubMed: 14699503]

Lamm ML, Catbagan WS, Laciak RJ, Barnett DH, Hebner CM, Gaffield W, Walterhouse D, Iannaccone P, Bushman W. Sonic hedgehog activates mesenchymal Gli1 expression during prostate ductal bud formation. Dev Biol 2002;249(2):349–366. [PubMed: 12221011]

Lee KL, Peehl DM. Molecular and cellular pathogenesis of benign prostatic hyperplasia. J Urol 2004;172 (5 Pt 1):1784–1791. [PubMed: 15540721]

Lipinski RJ, Cook CH, Barnett DH, Gipp JJ, Peterson RE, Bushman W. Sonic hedgehog signaling regulates the expression of insulin-like growth factor binding protein-6 during fetal prostate development. Dev Dyn 2005;233(3):829–836. [PubMed: 15906375]

Luo J, Duggan DJ, Chen Y, Sauvageot J, Ewing CM, Bittner ML, Trent JM, Isaacs WB. Human prostate cancer and benign prostatic hyperplasia: Molecular dissection by gene expression profiling. Cancer Res 2001;61(12):4683–4688. [PubMed: 11406537]

McNeal JE. Origin and evolution of benign prostatic enlargement. Invest Urol 1978;15(4):340–345. [PubMed: 75197]

McNeal J. Pathology of benign prostatic hyperplasia. Insight into etiology. Urol Clin North Am 1990;17 (3):477–486. [PubMed: 1695776]

Moolenaar WH, van Meeteren LA, Giepmans BN. The ins and outs of lysophosphatidic acid signaling. Bioessays 2004;26(8):870–881. [PubMed: 15273989]

Nam SW, Clair T, Kim YS, McMarlin A, Schiffmann E, Liotta LA, Stracke ML. Autotaxin (NPP-2), a metastasis-enhancing motogen, is an angiogenic factor. Cancer Res 2001;61(18):6938–6944. [PubMed: 11559573]

Nelson PS. Predicting prostate cancer behavior using transcript profiles. J Urol 2004;172(5 Pt 2):S28–S32. [PubMed: 15535439]discussion S33

Okada H, Danoff TM, Kalluri R, Neilson EG. Early role of Fsp1 in epithelial-mesenchymal transformation. Am J Physiol 1997;273(4 Pt 2):F563–F574. [PubMed: 9362334]

Peehl DM, Sellers RG. Cultured stromal cells: An in vitro model of prostatic mesenchymal biology. Prostate 2000;45(2):115–123. [PubMed: 11027410]

Rose A, Xu Y, Chen Z, Fan Z, Stamey TA, McNeal JE, Caldwell M, Peehl DM. Comparative gene and protein expression in primary cultures of epithelial cells from benign prostatic hyperplasia and prostate cancer. Cancer Lett 2005;227(2):213–222. [PubMed: 16112424]

Sala-Newby GB, George SJ, Bond M, Dhoot GK, Newby AC. Regulation of vascular smooth muscle cell proliferation, migration and death by heparan sulfate 6-O-endosulfatase1. FEBS Lett 2005;579 (28):6493–6498. [PubMed: 16289059]

San Francisco IF, DeWolf WC, Peehl DM, Olumi AF. Expression of transforming growth factor-beta 1 and growth in soft agar differentiate prostate carcinoma-associated fibroblasts from normal prostate fibroblasts. Int J Cancer 2004;112(2):213–218. [PubMed: 15352032]

Shapiro E, Becich MJ, Hartanto V, Lepor H. The relative proportion of stromal and epithelial hyperplasia is related to the development of symptomatic benign prostate hyperplasia. J Urol 1992;147(5):1293–1297. [PubMed: 1373778]

Sherlock G, Hernandez-Boussard T, Kasarskis A, Binkley G, Matese JC, Dwight SS, Kaloper M, Weng S, Jin H, Ball CA, Eisen MB, Spellman PT, Brown PO, Botstein D, Cherry JM. The Stanford microarray database. Nucleic Acids Res 2001;29(1):152–155. [PubMed: 11125075]

Song J, Clair T, Noh JH, Eun JW, Ryu SY, Lee SN, Ahn YM, Kim SY, Lee SH, Park WS, Yoo NJ, Lee JY, Nam SW. Autotaxin (lysoPLD/NPP2) protects fibroblasts from apoptosis through its enzymatic product, lysophosphatidic acid, utilizing albumin-bound substrate. Biochem Biophys Res Commun 2005;337(3):967–975. [PubMed: 16219296]

Stamey TA, Caldwell MC, Fan Z, Zhang Z, McNeal JE, Nolley R, Chen Z, Mahadevappa M, Warrington JA. Genetic profiling of Gleason grade 4/5 prostate cancer: Which is the best prostatic control tissue? J Urol 2003;170(6 Pt 1):2263–2268. [PubMed: 14634393]

Strutz F, Okada H, Lo CW, Danoff T, Carone RL, Tomaszewski JE, Neilson EG. Identification and characterization of a fibroblast marker: FSP1. J Cell Biol 1995;130(2):393–405. [PubMed: 7615639]

Tusher VG, Tibshirani R, Chu G. Significance analysis of microarrays applied to the ionizing radiation response. Proc Natl Acad Sci USA 2001;98(9):5116–5121. [PubMed: 11309499]

Tuxhorn JA, Ayala GE, Rowley DR. Reactive stroma in prostate cancer progression. J Urol 2001;166 (6):2472–2483. [PubMed: 11696814]

Tuxhorn JA, Ayala GE, Smith MJ, Smith VC, Dang TD, Rowley DR. Reactive stroma in human prostate cancer: Induction of myofibroblast phenotype and extracellular matrix remodeling. Clin Cancer Res 2002a;8(9):2912–2923. [PubMed: 12231536]

Tuxhorn JA, McAlhany SJ, Dang TD, Ayala GE, Rowley DR. Stromal cells promote angiogenesis and growth of human prostate tumors in a differential reactive stroma (DRS) xenograft model. Cancer Res 2002b;62(11):3298–3307. [PubMed: 12036948]

Umezu-Goto M, Kishi Y, Taira A, Hama K, Dohmae N, Takio K, Yamori T, Mills GB, Inoue K, Aoki J, Arai H. Autotaxin has lysophospholipase D activity leading to tumor cell growth and motility by lysophosphatidic acid production. J Cell Biol 2002;158(2):227–233. [PubMed: 12119361]

Wang S, Ai X, Freeman SD, Pownall ME, Lu Q, Kessler DS, Emerson CP Jr. QSulf1, a heparan sulfate 6-O-endosulfatase, inhibits fibroblast growth factor signaling in mesoderm induction and angiogenesis. Proc Natl Acad Sci USA 2004;101(14):4833–4838. [PubMed: 15051888]

West RB, Corless CL, Chen X, Rubin BP, Subramanian S, Montgomery K, Zhu S, Ball CA, Nielsen TO, Patel R, Goldblum JR, Brown PO, Heinrich MC, van de Rijn M. The novel marker, DOG1, is expressed ubiquitously in gastrointestinal stromal tumors irrespective of KIT or PDGFRA mutation status. Am J Pathol 2004;165(1):107–113. [PubMed: 15215166]

Zhao H, Lai F, Nonn L, Brooks JD, Peehl DM. Molecular targets of doxazosin in human prostatic stromal cells. Prostate 2005;62(4):400–410. [PubMed: 15378519]

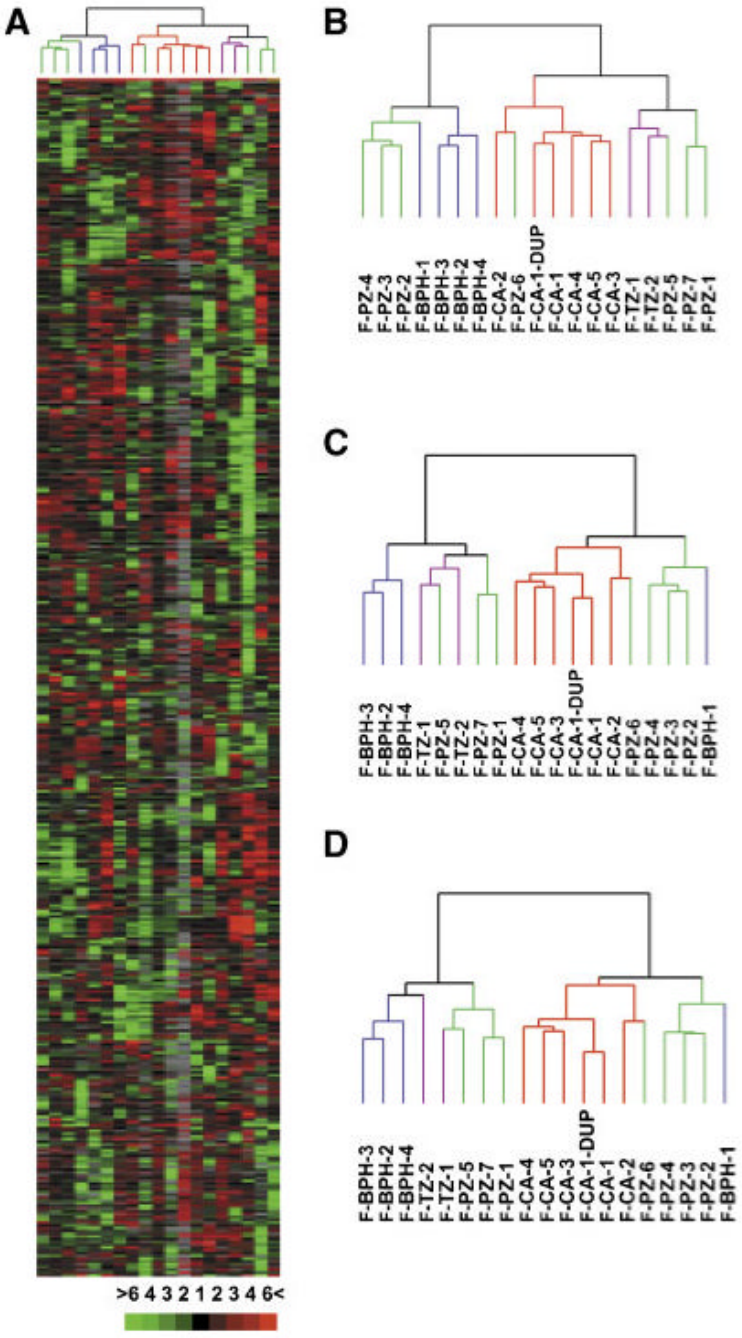

Fig. 1.

Hierarchical clustering analysis of genes differentially expressed in prostatic stromal cells. **A**: Overview of relative expression levels of 714 genes represented by 1,032 clones whose expression varied at least threefold from the mean abundance in at least three samples in all 18 stromal cell cultures. Each column represents data from a single stromal cell culture, and each row represents expression levels for a single gene across the 18 samples. Transcripts upregulated were in red and downregulated in green. The degree of color saturation corresponds with the ratio of gene expression shown at the bottom of the image. Full transcript identities and raw data are available at http://www.Stanford.edu/~hongjuan/stromal. In the dendrogram shown on top of the image, BPH cells were colored in blue, CA cells in red, PZ cells in green,

and TZ cells in purple. The same color code was used in (**B-D**). B: Dendrogram of clustering analysis using the 1,032 clones described in (A). C: Dendrogram of clustering analysis using 455 clones representing 361 genes whose expression varied at least threefold from the mean abundance in at least four samples in all 18 stromal cell cultures. D: Dendrogram of clustering analysis using 232 clones representing 192 genes whose expression varied at least fourfold from the mean abundance in at least four samples in all 18 stromal cell cultures. [Color figure can be viewed in the online issue, which is available at www.interscience.wiley.com.]

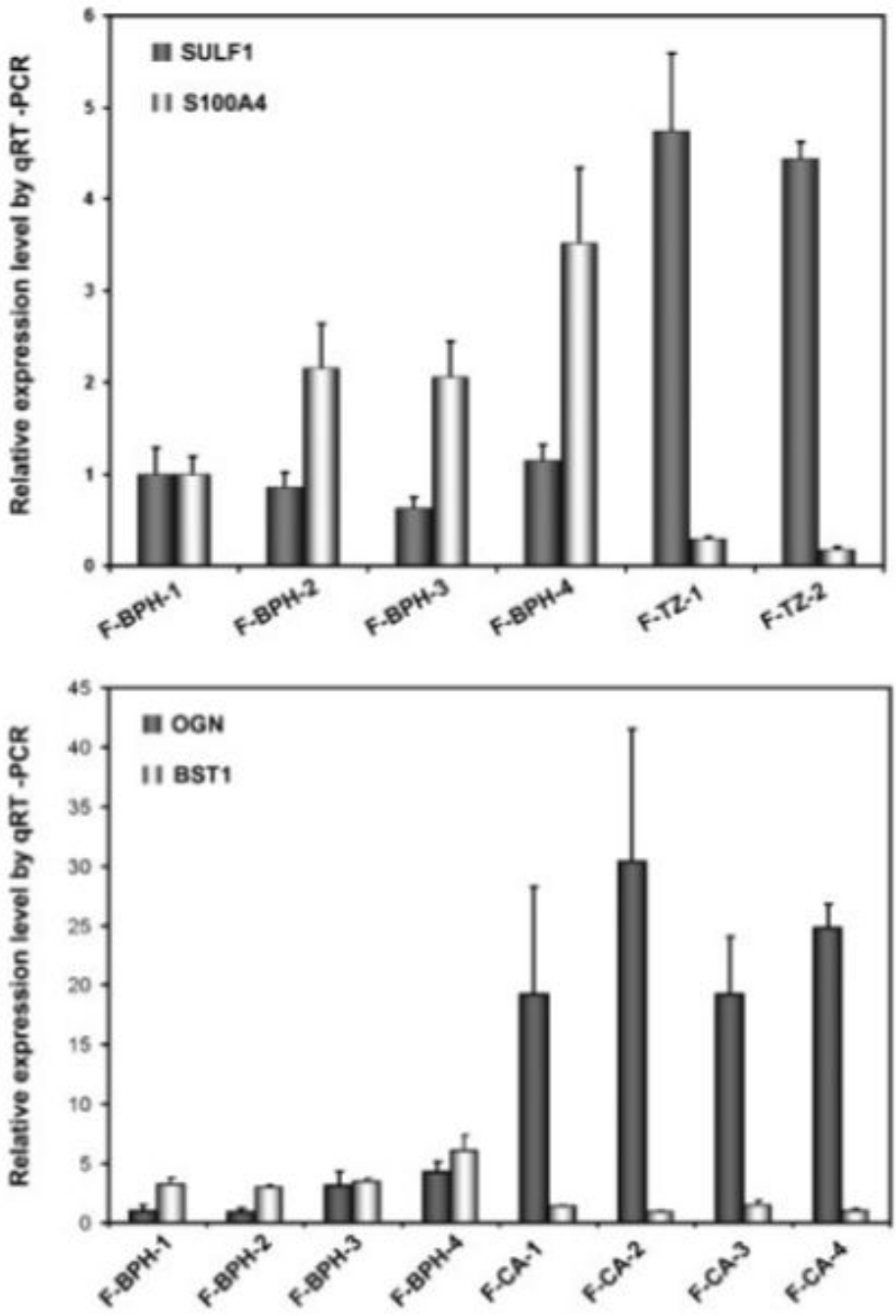

Fig. 2.

Validation of gene expression changes observed using microarray by real-time RT-PCR. Levels of transcripts of interest determined by PT-PCR in triplicates were normalized against that of TBP in the same sample. For comparison, expression levels in F-BPH-1 were scaled to 1, except for BST1, for which expression level in F-CA-4 was scaled to 1.

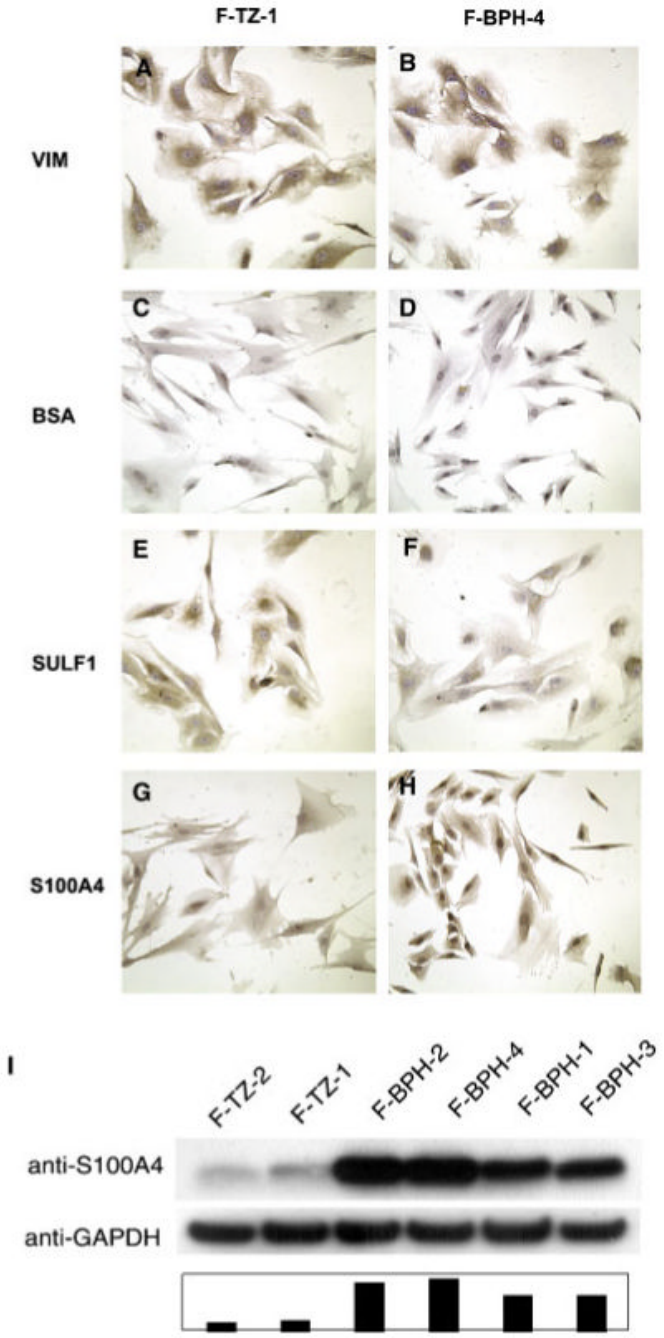

Fig. 3.

Comparison of SULF1 and S100A4 expression in cultured BPH and TZ cells by immunochemistry (**A-H**) and Western blotting (**I**). SULF1 expression is significantly less in F-BPH-4 cells (E) compared to F-TZ-1 cells (F), whereas S100A4 expression is much higher in F-BPH-4 cells (G) than in F-TZ-1 cells (H). Both cell cultures showed similar uniform expression of vimentin (A, B) and no staining when BSA was used as negative control (C, D). Western blotting (I) showed S100A4 expression was decreased in BPH cells, ranging from 7.7- to 10.7-fold, compared to TZ cells. [Color figure can be viewed in the online issue, which is available at www.interscience.wiley.com.]

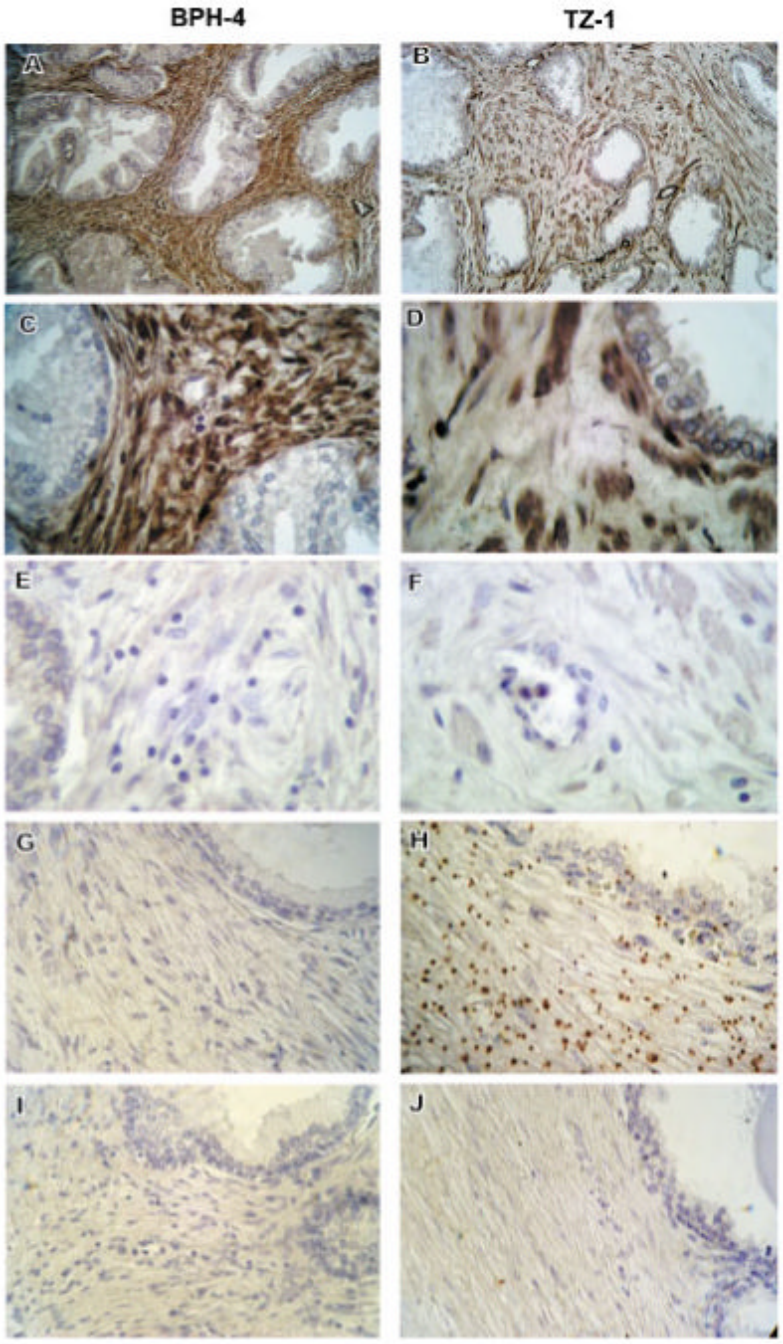

Fig. 4.

Comparison of S100A4 and SULF1 expression in tissue sections of BPH and TZ. Intense staining of S100A4 by immunohistochemistry was observed throughout the stromal area of BPH tissue from which the cell culture, F-BPH-4, was derived (**A**), whereas only some stromal cells showed expression of S100A4 in the normal TZ tissue from which F-TZ-1 was derived (**B**). **C** and **D** are higher magnification of (A) and (B), respectively. **E** and **F** are negative controls stained with BSA. In situ hybridization using anti-sense RNA probe against SULF1 showed that SULF1 transcript is present at high levels in the stroma of normal TZ tissue (**H**), but not in BPH stroma (**G**), whereas sense RNA probe did not show labeling in either BPH

(**I**) or TZ (**J**) stroma. [Color figure can be viewed in the online issue, which is available at www.interscience.wiley.com.]

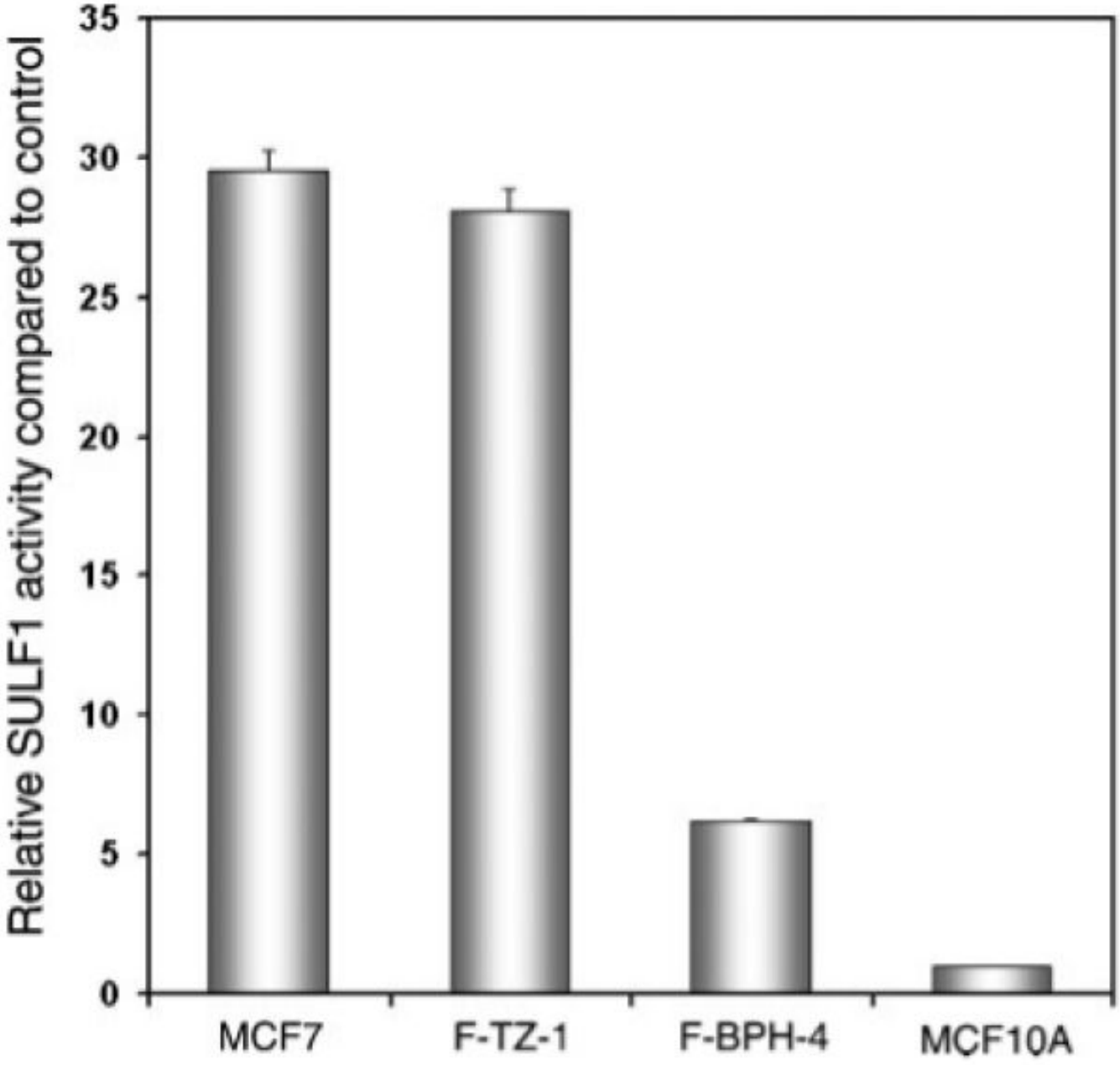

Fig. 5.

Sulfatase assay in cultured BPH and TZ stromal cells. Relative activity was calculated by scaling the activity in MCF-10A cells, the negative control, to 1. MCF-7 cells were used as a positive control. F-BPH-4 cells showed a more than fourfold decrease in SULF1 activity compared to F-TZ-1 cells.

TABLE 1

Summary of cell cultures used in the study

Name	Age of donor	Passage number	Histology
F-BPH-1	63	10	BPH
F-BPH-2	55	11	BPH
F-BPH-3	65	14	BPH
F-BPH-4	58	8	BPH
F-TZ-1	43	16	Normal TZ
F-TZ-2	62	14	Normal TZ
F-CA-1	57	11	CA 4/3
F-CA-2	69	10	CA 3/4
F-CA-3	58	10	CA 3/4
F-CA-4	59	14	CA 3/3
F-CA-5	65	14	CA 4/3
F-PZ-1	67	15	Normal PZ
F-PZ-2	58	16	Normal PZ
F-PZ-3	66	11	Normal PZ
F-PZ-4	66	4	Normal PZ
F-PZ-5	59	11	Normal PZ
F-PZ-6	66	15	Normal PZ
F-PZ-7	59	17	Normal PZ

TABLE 2

Genes differentially expressed in BPH compared to TZ stromal cells identified by SAM

Symbol	Fold change	SAM rank	GO annotation
Downregulated in BPH			
SULF1	-3.8	1	Apoptosis
TGFB2	-4.2	2	Cell proliferation/cell cycle
LASS6	-5.0	3	Regulation of transcription
Upregulated in BPH			
S100A4	10.8	1	Calcium ion binding
TOX	34.2	2	Regulation of transcription
BUB1	19.7	3	Cell cycle/cell proliferation
CLDN23	6.0	7	Cell-cell adhesion
OAS2	6.7	8	Immune response
IF	5.4	9	Immune response
GBP2	15.3	11	Immune response
DNAJC4	3.0	12	Protein folding
GLI3	45.8	13	Regulation of transcription/signal transduction
SOX12	3.6	14	RNA polymerase II transcription factor activity
AIM1	6.6	15	Sugar binding
DKFZP586A0522	5.0	16	Methyltransferase activity
S100A10	4.9	17	Calcium ion binding
PLGL	5.8	19	Plasmin activity
PLEKHC1	3.2	20	Cell adhesion
RPS6KL1	3.2	22	Structural constituent of ribosome
TEAD3	2.8	25	Regulation of transcription
BST1	2.8	28	Humoral immune response

TABLE 3

Genes differentially expressed in BPH compared to CA stromal cells identified by SAM

Symbol	Fold change	SAM rank	GO annotation
Upregulated in CA			
BACE2	5.0	1	Peptide hormone processing
SULF1	4.4	2	Apoptosis
OGN	7.1	3	Growth factor activity
MGP	2.3	4	Cell differentiation
DOCK10	4.4	5	Guanyl-nucleotide exchange factor activity
THY1	3.4	6	Cell surface antigen
Upregulated in BPH			
BST1	4.2	1	Humoral immune response
ARHGAP28	3.8	2	Viral release
OLR1	2.3	3	Proteolysis and peptidolysis
COL4A5	5.0	4	Extracellular matrix structural constituent
TOX	5.0	6	Regulation of transcription
IGF-2	10.2	7	Cell proliferation/regulation of cell cycle
SLC6A6	6.1	8	Taurine:sodium symporter activity
TEK	6.4	9	Cell-cell signaling/signal transduction
KMO	2.5	10	Electron transport
C11orf30	2.0	11	DNA repair/regulation of transcription
LOC492304	6.7	12	Insulin-like growth factor binding
TBL1X	2.5	14	Regulation of transcription
CHN1	3.7	15	GTPase activator activity
SLC4A4	5.7	16	Sodium:bicarbonate symporter activity
MFHAS1	2.3	17	Small GTPase mediated signal transduction
TERF1	2.0	18	Cell cycle/regulation of transcription
FARP1	2.1	19	Rho guanyl-nucleotide exchange factor activity
MPP3	3.5	20	Guanylate kinase activity/signal transduction
VAMP5	2.8	21	Cell differentiation/vesicle-mediated transport
SSH2	2.2	22	Protein amino acid dephosphorylation
GTF2E1	1.9	24	Regulation of transcription
SIPA1L2	2.6	27	GTPase activator activity
NRG2	6.4	28	Anti-apoptosis/cell-cell signaling
MYO6	2.0	29	ATPase activity/structural constituent of muscle

TABLE 4

Genes upregulated in CA compared to PZ stromal cells identified by SAM

Symbol	Fold change	SAM rank	GO annotation
ENPP2	7.4	1	Chemotaxis/transcription factor binding
TM4SF3	3.6	2	Signal transducer activity
SEPT6	3.7	6	Cell cycle
ICAM4	2.3	8	Cell-cell adhesion
LOC91431	1.8	12	Zinc ion binding
ADCK1	2.4	13	Protein amino acid phosphorylation
DLL3	3.3	15	Cell fate determination
CMRF35	2.9	16	Cellular defense response
P2RY1	1.8	18	G-protein signaling
LRRC7	2.0	19	Protein binding
DYRK2	1.9	21	Protein amino acid phosphorylation
LOC400713	1.9	22	Regulation of transcription
WDR7	2.2	23	Cell cycle/apoptosis
NAGA	2.9	25	Carbohydrate metabolism
NF1	2.3	27	Ras protein signal transduction/cell cycle
C16orf34	2.4	28	Regulation of transcription
HSPD1	2.0	29	Response to unfolded protein
MICAL2	2.3	30	Electron transport
C6orf68	2.4	31	Metabolism | transferase activity
IGF-1	1.9	32	Positive regulation of cell proliferation
BCL2A1	2.5	34	Anti-apoptosis
CRY1	2.1	36	DNA repair/G-protein coupled photoreceptor activity
FRAG1	1.6	37	Receptor activity
NISCH	1.7	38	Intracellular signaling cascade
FBXW8	2.1	39	Ubiquitin cycle
TRIM33	1.7	40	Regulation of transcription/ubiquitin-protein ligase activity
PDE3B	2.0	41	Signal transduction
LMO2	4.4	42	Zinc ion binding
SLC5A8	1.8	45	Transporter activity
UGT2B7	4.2	49	Lipid metabolism

Symbol	Fold change	SAM rank	GO annotation
MCM5	2.6	51	Regulation of cell cycle/regulation of transcription
TAC1	2.7	52	Cell-cell signaling
SPRY3	2.0	54	Regulation of signal transduction
LTB4R	1.8	55	Inflammatory response/signal transduction
PKIB	3.7	56	cAMP-dependent protein kinase inhibitor activity
KCTD13	1.8	59	Voltage-gated potassium channel activity
ATF6	1.8	64	Regulation of transcription/signal transduction
EBF	1.9	65	Regulation of transcription
MARCH-I	2.2	66	Protein ubiquitination
PANX2	1.7	67	Gap junction
FLJ22405	2.2	68	Protein amino acid dephosphorylation
LGR4	1.9	69	G-protein coupled receptor protein signaling pathway
XAB1	2.3	71	Small GTPase mediated signal transduction
CA12	2.7	72	One-carbon compound metabolism
MUC5B	1.9	74	Cell adhesion
RERG	1.9	75	Cell proliferation/signal transduction
LOC126295	1.7	76	Regulation of transcription
GATA6	3.7	77	Regulation of transcription
FGFR1	1.9	78	Cell growth/FGF receptor signaling pathway
ARGBP2	2.1	79	Structural constituent of muscle
ERBB2	1.8	81	Cell proliferation
COL4A2	1.9	83	Cell adhesion
NUP160	2.0	84	mRNA-nucleus export
LIMS3	3.2	85	Zinc ion binding
AKR1B10	2.1	86	Aldehyde metabolism/electron transporter
OGN	1.9	88	Growth factor activity
NRK	1.9	89	Small GTPase regulator activity
RPL27A	1.8	91	Structural constituent of ribosome
TRPM3	1.7	92	Calcium ion transport
DCAMKL1	5.8	93	Cell differentiation
KCNIP4	1.7	94	Calcium ion binding
KCNC4	3.8	95	Cation transport

Symbol	Fold change	SAM rank	GO annotation
IGSF10	1.9	97	Vascular endothelial growth factor receptor activity
GSTZ1	1.8	98	Tyrosine catabolism
ZNF367	2.1	99	Nucleic acid binding
PON1	5.8	100	Aryldialkylphosphatase activity
HSPB6	3.0	101	Response to unfolded protein

TABLE 5

Validation of gene expression by qRT-PCR

Symbol	Fold change	SAM rank	*P*-value (≤0.05)
BPH versus TZ			
SULF1	↓5.1	↓1	Yes
TGFB2	↓1.4	↓2	No
LASS6	↓5.1	↓3	Yes
S100A4	↑9.3	↑1	Yes
TOX	↑5.5	↑2	Yes
BUB1	↑3.4	↑3	No
CLDN23	↑4.6	↑7	Yes
OAS2	↑2.0	↑8	No
IF	↑5.3	↑9	Yes
GBP2	↑11.6	↑11	Yes
DNAJC4	↑1.1	↑12	No
GLI3	↑9.4	↑13	Yes
S100A10	↑5.5	↑17	Yes
BST1	↑1.4	↑28	No
BPH versus CA			
SULF1	↓4.6	↓2	No
OGN	↓10.0	↓3	Yes
THY1	↓3.8	↓6	Yes
BST1	↑3.3	↑1	Yes
TOX	↑3.4	↑6	Yes
IGF-2	↑9.9	↑7	Yes
LOC492304	↑9.6	↑12	Yes
CA versus PZ			
ENPP2	↑2.7	↑1	Yes
TM4SF3	↑8.3	↑2	Yes
SEPT6	↑3.5	↑6	Yes
ICAM4	↑2.7	↑8	Yes
LOC91431	1.0	↑12	No
ADCK1	↓1.4	↑13	No
DLL3	↓1.4	↑15	No
WDR7	↑1.5	↑23	Yes
IGF-1	↑2.7	↑32	No
BCL2A1	↑9.4	↑34	No
FRAG1	↓1.1	↑37	No
FGFR1	↑2.0	↑78	Yes
OGN	↑5.8	↑88	Yes
PON1	↓2.0	↑100	No